

Polarization characteristics of a reflective erbium doped fiber amplifier with temperature changes at the Faraday rotator mirror

M. Angeles Quintela, José Miguel López-Higuera and César Jáuregui

*Grupo de Ingeniería Fotónica –Universidad de Cantabria
E.T.S.I.I. y Telecomunicación – Dpto. TEISA
Avda. Los Castros s/n – c.p. 39005 Santander, Spain
Tel: ++ 34-942-200879; Fax: ++ 34-942-200877
quintela@teisa.unican.es*

Abstract: The temperature dependence of a Faraday rotator mirror (FRM) used in a reflective erbium doped fiber amplifier (R-EDFA) is reported in this paper. The influence of this dependence on the polarization state (PS) of amplified optical signals is also discussed.

©2005 Optical Society of America

OCIS codes: (060.2320) Fiber optics amplifiers and oscillators; (260.5430) Polarization; (160.3820) Magneto-optical materials.

References and Links

1. Govind P. Agrawal, *Fiber-Optic Communication Systems (Third Edition)*, Ed. (Wiley & Sons, New York, 2002).
2. J.M. López-Higuera, *Handbook of Optical Fiber sensing Technology*, Ed. (Wiley & Sons, Chichester, 2002).
3. J.C. Dung, S. Chi, C.C. Chen, "Characteristics of the erbium doped fiber amplifier with polarization mode dispersion compensation," *Opt. Commun.*, **222**, 207-212 (2003).
4. S. Yamashita, K. Hotate, M. Ito, "Polarization properties of a reflective fiber amplifier employing a circulator a faraday rotator mirror," *J. Lightwave Technol.*, **13**, 385-389 (1996).
5. M. Martinelli, "A universal compensator for polarization changes induced by birefringence on retracing beam," *Opt. Commun.*, **72**, 341-344 (1989).
6. Y. Honda, T. Hibiya and K. Shiroki, "DyBi garnet films with improved temperature dependence of Faraday rotation," *IEEE Trans. J. Magnet. Jpn.* **TJMJ-2**, 142-144 (1987).
7. R. C. Jones, "A new calculus for the treatment of optical systems," *J. Opt. Soc. Am.* **31**, 488-503, (1941).
8. M. A. Quintela, C. Jauregui, F. J. Madruga, J.M. López-Higuera, "Experimental characterization of light polarization in active erbium doped fiber," *Microwave Opt. Technol. Lett.*, **42**, 395-397 (2004).
9. M. A. Quintela, C. Jauregui, O. M. Conde, A. M. Cubillas, J.M. López-Higuera, "Optical signal polarization state instability on erbium doped fibers," in *Second European Workshop on Optical Fibre Sensors*, Proc. SPIE **5502**, 544-547 (2004).
10. E. Desurvire, D. Bayart, B. Desthieux, S. Bigo, *Erbium-doped fiber amplifiers (Device and system developments)*, Ed. (Wiley & Sons, New York, 2002).

1. Introduction

Erbium Doped Fiber (EDF) has attracted attention in both sensing and telecommunication fields. This is due to its excellent characteristics for optical amplification. The behavior of the polarization state (PS) of the light in EDFs must be kept in mind because its influence on the characteristics of the system is very important. In digital optical fiber communications, EDF polarization phenomena [1] are important limiting factors to high-speed long-distance systems. These so-called polarization phenomena include polarization mode dispersion (PMD), polarization hole burning (PHB), polarization-dependent gain (PDG) and

polarization-dependent loss (PDL). Fluctuations in the PS of the optical signal [2] can degrade the quality of the measurements made with optical fiber sensors. This is especially true for those techniques based on interferometry and polarimetry, where an EDF can be used to enhance both sensitivity and accuracy.

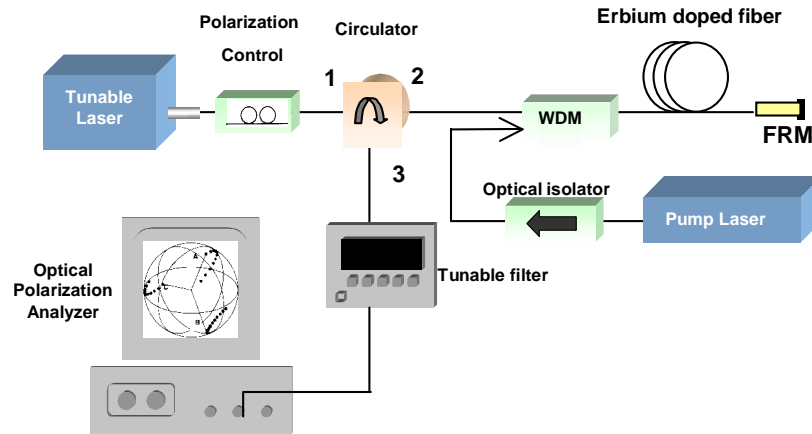


Fig. 1. General measurement set-up used in this research work.

Different techniques have been developed to improve the polarization behavior of light in erbium doped fiber amplifiers (EDFA). The use of a Faraday rotator mirror (FRM) at the end of the EDF is the most popular technique to stabilize the PS [3, 4]. This amplifier configuration is known as reflective erbium doped fiber amplifier (R-EDFA). Faraday rotator mirrors consist in a 45° Faraday rotator (based on the Faraday effect) and a mirror [5]. These FRMs have the peculiarity that the PS of the reflected (backward) optical signal is orthogonal to the PS of the forward optical signal. Furthermore, this PS is, in theory, independent of the birefringence of the optical system. As a consequence the output PS is preserved regardless of the external perturbations and, therefore, is not affected by polarization phenomena.

In general commercial Faraday rotators are made of ferromagnetic materials: yttrium iron garnet (YIG) or bismuth-substituted iron garnet (BIG). The magneto-optical properties of these ferromagnetic materials show great temperature dependence. The reason for this is to be found in the temperature dependence of the saturation magnetization. In crystals with a ferromagnetic garnet structure the saturation magnetization is the vectorial sum of magnetization of three sub-lattices corresponding to three magnetic ion crystallization sites (tetrahedron, octahedron and dodecahedron). Therefore, changing each magnetization contribution of the sub-lattices to the sum of saturation magnetization, or changing the quantity and types of the substituted ions or rare-earth ions in the sub-lattices, the temperature dependence of the Faraday rotation can be modified. Thus, small variations of the rotation angle can take place in the 45° Faraday rotator when it suffers temperature changes [6]. However, the temperature sensitivities are different depending on the ferromagnetic material of the rotator. This temperature dependence has a negative influence on the capabilities of compensation of polarization changes provoked by externally-induced birefringence on a R-EDFA. To our knowledge this is the first time that the FRM temperature-dependence influence on the polarization behavior of the optical signal in a R-EDFA has been specifically studied and experimentally demonstrated.

This paper is organized as follows: first a theoretical study is carried out, later on several experimental results are presented and discussed and, finally, some conclusions are extracted.

2. Theory

The R-EDFA configuration can be extracted from the general measurement set-up used in this work, which is shown in Fig. 1. The optical signal is launched into the EDF through an optical circulator and a wavelength division multiplexing (WDM). The amplified signal, after being reflected at the FRM, is amplified again and is extracted from the port 3 of the optical circulator. That is, the R-EDFA input and output are the circulator ports number 1 and 3, respectively.

Jones matrices have been used in this work to analyze polarization properties of the R-EDFA. Jones matrices for both forward (T_F) and backward (T_B) directions in the EDF have been calculated neglecting polarization-dependent losses [7]. They are given by:

$$\begin{aligned} T_F &= g \begin{bmatrix} a & b \\ -b^* & a^* \end{bmatrix} \\ T_B &= g \begin{bmatrix} a & b^* \\ -b & a^* \end{bmatrix} \end{aligned} \quad (1)$$

where a and b are complex values depending on the birefringence of the EDF and g is the average gain (including losses).

The Jones matrix of the FRM is defined as

$$T_{FRM} = \gamma \begin{bmatrix} \sin 2\Delta\vartheta & -\cos 2\Delta\vartheta \\ -\cos 2\Delta\vartheta & -\sin 2\Delta\vartheta \end{bmatrix} \quad (2)$$

where $\Delta\vartheta$ is the rotation angle maladjustment with respect to the 45° rotation angle of the Faraday rotator.

The only component remaining to be modeled with a Jones matrix is the circulator. Since a polarization independent circulator has two optical paths there will be a phase delay (Δ) between these paths. Thus the Jones matrices that describe the transmission from port 1 to port 2 (T_{12}) and from port 2 to port 3 (T_{23}) of a polarization independent circulator are expressed, respectively, as

$$\begin{aligned} T_{12} &= \gamma_c \begin{bmatrix} 0 & -\beta^* \\ \beta & 0 \end{bmatrix} \\ T_{23} &= \gamma_c \begin{bmatrix} -\beta^* & 0 \\ 0 & \beta \end{bmatrix} \end{aligned} \quad (3)$$

where $\beta = e^{i\Delta/2}$ and γ_c is the circulator loss. It is assumed that the losses are the same for the two paths.

The Jones matrices of the EDF in the forward and backward direction (T_F and T_B), the Jones matrices of the FRM (T_{FRM}) and the circulator (T_{12} and T_{23}) can be then multiplied by to obtain the complete PS behavior of the light going out the amplifier. Thus, the Jones matrix of the complete amplifier (T_{R-EDFA}) is:

$$T_{R-EDFA} = T_{23} \cdot T_B \cdot T_{FRM} \cdot T_F \cdot T_{12} \quad (4)$$

Therefore, after some mathematical manipulation, T_{R-EDFA} becomes

$$T_{R-EDFA} = g^2 \gamma_c^2 \cos(2\Delta\vartheta) T_U + g^2 \gamma_c^2 \sin(2\Delta\vartheta) T_M \quad (5)$$

where T_U is a unit matrix and T_M is a Jones matrix accounting for the rotation angle maladjustment due to the temperature dependence of the magneto-optical Faraday effect:

$$T_U = \begin{bmatrix} 1 & 0 \\ 0 & 1 \end{bmatrix} \quad (6)$$

$$T_M = \begin{bmatrix} p & q \\ -q & -p \end{bmatrix}$$

Here $p = -ab + a^*b^*$, $q = \beta^{*2}(a^2 + b^{*2})$ and $|p|^2 + |q|^2 = 1$.

Applying the T_{R-EDFA} matrix to an arbitrary input PS in the case of using an ideal FRM ($\Delta\vartheta=0$), it can be demonstrated that the output PS is preserved regardless of the external perturbations. As a consequence, in these ideal circumstances this optical amplifier configuration is immune to any polarization phenomena (PMD, PHB, PDG and PDL). However, it is rather difficult to obtain an accurate 45° rotation angle with the Faraday rotator. Moreover, temperature changes at the FRM play an important role in the rotation angle maladjustment.

A figure of merit should be defined [4] to theoretically evaluate the influence of the rotation angle maladjustment on the polarization behavior of the amplified optical signal. This figure of merit is the extinction ratio (r). It relates the amount of output optical power of the desired PS (parallel to the input PS) to that of the unwanted PS (perpendicular to the input PS). The desired PS is parallel to the input PS because, in the ideal case ($\Delta\vartheta=0$), this fiber amplifier preserves the input PS, as can be seen in ec. (5). Being \vec{E}_{\parallel} the Jones vector of the input signal, the Jones vector of the output signal can be decomposed in two terms: one parallel to \vec{E}_{\parallel} (polarization behavior with an ideal FRM) and another one that can be expressed as a linear combination of \vec{E}_{\parallel} and its orthogonal vector \vec{E}_{\perp} . This last component is a product of the influence of temperature on the rotation angle of the Faraday rotator. Therefore, the extinction ratio r , that relates \vec{E}_{\parallel} (desired) and \vec{E}_{\perp} (unwanted), is given by

$$r = \frac{E_{\parallel}}{E_{\perp}} \frac{|\cos(2\Delta\vartheta) + u \sin(2\Delta\vartheta)|^2}{|v \sin(2\Delta\vartheta)|^2} \quad (7)$$

where:

$$u = \left(T_M \vec{E}_{\parallel} \cdot \vec{E}_{\parallel} \right) \quad (8)$$

$$v = \left(T_M \vec{E}_{\parallel} \cdot \vec{E}_{\perp} \right)$$

The complex values u and v are calculated as the inner products of \vec{E}_{\parallel} and T_M , and \vec{E}_{\perp} and T_M respectively.

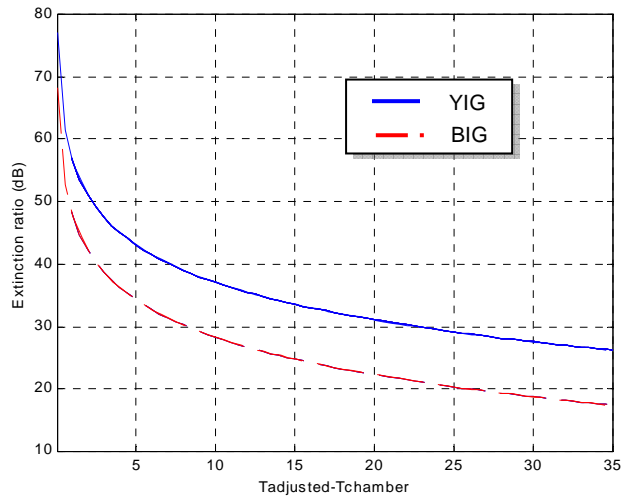


Fig. 2. Minimum extinction ratio for two FRM's: YIG(solid blue line) and BIG (dotted red line) as a function of the temperature deviation from the one at which the Faraday rotator was adjusted to 45°.

The minimum extinction ratio r_{\min} (worst case) is then given by:

$$r_{\min} = \frac{1}{[\tan(2\Delta\vartheta)]^2} \quad (9)$$

Figure 2 shows the minimum extinction ratio for two FRMs (whose Faraday rotators are made of YIG and BIG materials respectively) as a function of the temperature deviation from the temperature at which the Faraday rotator was adjusted to 45° (T_{adjusted}). The temperature dependence of $\Delta\vartheta$ is approximately 0.04 deg/°C for YIG and 0.11 deg/°C for BIG [6]. From Fig. 2, a reduction of the extinction ratio as temperature increases can be observed. To get a minimum extinction ratio of 40 dB (typical value for commercial FRMs), the allowable temperature increment is 7°C in commercial FRM-YIGs and only 2.5°C in commercial FRM-BIGs. In short, the mentioned temperature-dependencies of the extinction ratio coefficient represent PS changes of the output optical signal of the R-EDFA. In the following, the latter will be experimentally checked.

3. Experimental results

The extinction ratio coefficient was used to theoretically demonstrate the PS changes of the optical signal induced by temperature fluctuations at the FRM. Nevertheless, the actual \vec{E}_{\parallel} and \vec{E}_{\perp} fields at the input and output at the amplifier (port 1 and 3 of the circulator, respectively) and their time stability are very difficult to be experimentally measured. Thus, as the main purpose of this work is to demonstrate the existence of the above mentioned PS changes, another figure of merit was used: the PS variance. This parameter is useful for measuring the PS fluctuations of an optical signal, as has recently been demonstrated by the authors [8] [9]. In the present work it is used to experimentally quantify the PS changes of the R-EDFA output optical signal.

On a Poincaré sphere the PS variance (σ_{PS}^2) is defined as the average of the azimuth variance (σ_{AZI}^2) and the ellipticity variance (σ_{ELLIP}^2) of the changing PS. These parameters are determined by [8] [9]:

$$\sigma_{AZI}^2 = \frac{1}{N} \cdot \sum_{i=1}^N (x_i - \eta_{AZI})^2 \quad (10)$$

$$\sigma_{ELLIP}^2 = \frac{1}{N} \cdot \sum_{i=1}^N (y_i - \eta_{ELLIP})^2 \quad (11)$$

where N is the number of measured points, x_i and y_i are, respectively, the azimuth and ellipticity values of the PS at each measurement time (T_i). On the other hand, η_{AZI} and η_{ELLIP} are the azimuth and ellipticity averages of the N PS's recorded during the experiment. All the measurements of this work have been carried out with $N = 3000$ over periods of 30 seconds.

In order to measure the PS variance the experimental set-up shown in Fig. 1 was used. The optical signal from the tunable laser (HP-8168F) went through a polarization control device before being launched into the R-EDFA input (circulator port 1). The R-EDFA output (circulator port 3) was connected to an optical polarization analyzer (OPA) (HP-8509B). A tunable filter is additionally used to decrease the optical noise of the amplifier.

A 26 meter-long erbium doped fiber (EDF) with an absorption peak of 5dB/m (which corresponds to a Er+3 concentration 300ppm at the core) was employed. The FRM used was a commercial ISOWAVE FRM made of YIG material. The FRM was put in a climatic chamber and the temperature was varied from 30°C to 65°C. The input signal had a wavelength of 1550 nm and a power of -5dBm. The EDF was pumped by a 1480 nm pump laser with a power of 17.6 dBm.

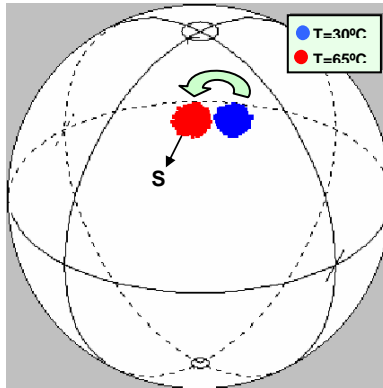


Fig. 3. Evolution of the PS of the amplified signal for a FRM temperature of 30°C (blue surface) and for a FRM temperature of 65°C (red surface). S is the area drawn on the Poincaré sphere by the changing PS in 30 seconds.

A sample of the results obtained for a FRM temperature of 30°C and 65°C are shown in Fig. 3. The PS random fluctuations of the output optical signal can be observed on the Poincaré sphere. The output optical signal had always a high degree of polarization, that is, it was above 90%. The PS variations were quantified with the aid of the PS variance ($\sigma_{PS}^2=6 \cdot 10^{-4}$ and $\sigma_{PS}^2=7 \cdot 10^{-4}$ for a FRM temperature of 30°C and 65°C respectively). As can be observed, the PS random fluctuations of the output optical signal were similar for both FRM temperatures (the surface S on the Poincaré sphere had the same diameter). Consequently the PS variances were also similar for both FRM temperatures.

These fluctuations can be explained by the fact that during the amplification process some photons are spontaneously emitted with random phase, random direction and random PS. During its propagation through the EDF these random photons are replicated through a stimulated emission process, in a similar fashion as the photons of the input light [10]. As a consequence, it can be stated that this amplified spontaneous emission (ASE) is a big deal responsible for the instabilities of the PS of the amplified optical signal. This also explains that the PS variances at both temperatures were similar. The gain and ASE of the R-EDFA were almost identical for these two FRM temperatures because the EDF was at a fixed temperature of 22°C. Although in this work the measurements have been carried out at 1550 nm (the FRM was designed to work at this wavelength), it should be pointed out that the PS variance is wavelength-dependent due to its direct relation with the ASE and gain of the R-EDFA. The PS variance, the gain and the ASE present maximums and minimums at the same wavelengths. Maximums around 1555 nm and minimums around 1570 nm and 1540 nm, respectively [8] [9].

Nevertheless, a movement of the S surface on the Poincaré sphere can be observed in Fig. 3. As was theoretically predicted by the extinction ratio coefficient, this movement of the S surface represents the change of the PS of the output optical signal due to the FRM temperature change. The movement of the S surface on the Poincaré sphere with respect to that corresponding to the initial temperature ($T=30^{\circ}\text{C}$) was also measured with the PS variance. In this case the azimuth and ellipticity variances of the changing PS were calculated at each temperature with respect to the azimuth and ellipticity averages of the PS at the initial temperature.

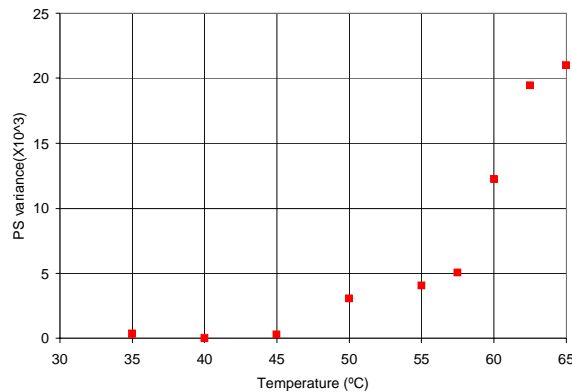


Fig. 4. PS variance as a function of FRM temperature. This PS variance quantify the change of the PS of the output optical signal.

Experimental measurements of this PS variance for temperatures ranging from 30°C to 65°C are shown in Fig. 4. In this graph the PS variance at the initial FRM temperature ($T=30^{\circ}\text{C}$) was subtracted from the PS variances of the other temperatures. From the figure, it can be deduced that the PS variance and, consequently, the change of the PS of the output optical signal increase with FRM temperature. These experimental results are in good agreement with those theoretically obtained from the extinction ratio coefficient.

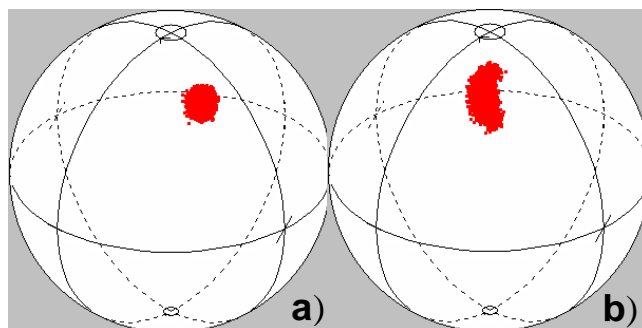


Fig. 5. Evolution of the PS of the amplified signal with perturbations applied to the EDF-coil: a) at a FRM temperature of 30°C, b) at a FRM temperature of 65°C.

The most important characteristic of the R-EDFA is its capacity to stabilize the PS of the output optical signal when externally-induced birefringences are present. However, the influence of the FRM temperature-dependence on the polarization has a negative effect on this characteristic of the R-EDFA. To experimentally verify this assertion, external perturbations were applied to an EDF section in order to induce linear birefringence. These external perturbations were induced by attaching a 8-turn 6-cm-diameter EDF coil to a fix holder placed on top of a TIRA vib 5100 shaker.

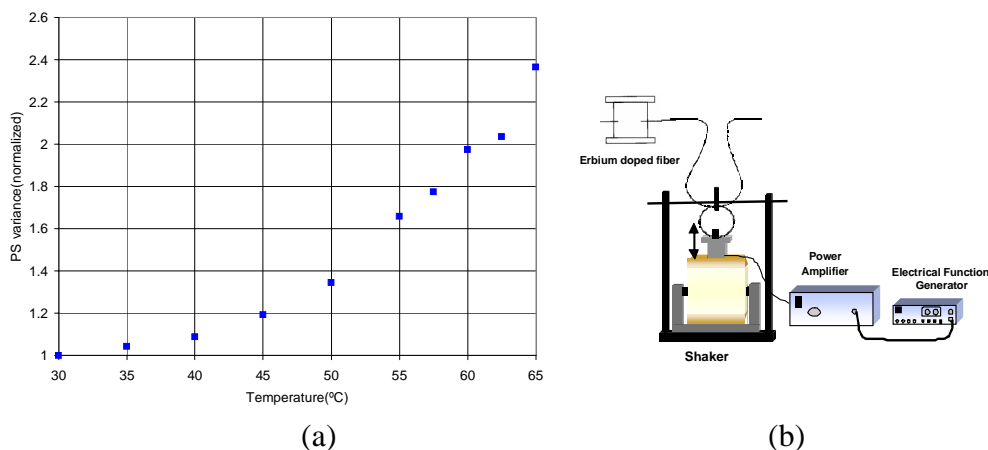


Fig. 6. (a) PS variance as a function of FRM temperature when the EDF was perturbed. (b) Illustration of the EDF coil deformation mechanism used to induce linear birefringence changes

Measurements of the PS variations of the output optical signal on the Poincaré sphere with perturbations applied to the EDF-coil for a FRM temperature of 30°C and 65°C are shown in Fig. 5(a) and Fig. 5(b), respectively. From Fig. 5(a) it can be seen that the PS of the output optical signal didn't suffer a substantial change with respect to the results of the same experiment but without perturbations (Fig. 3(a)). It can be seen that there was only a slight increment of the surface S on the Poincaré sphere when the system was perturbed. This might be due to a non-exactly 45° rotation angle. The results suggest that the FRM effectively cancels the effects of the linear birefringence. They also suggest that the PS variations of the output optical signal are exclusively caused by the ASE of the R-EDFA at this temperature.

On the other hand, the PS of the output optical signal changed sharply when the EDF was perturbed and the FRM temperature was 65°C (Fig. 5(b)). It can be observed that this externally-induced linear birefringence provoked important changes in the ellipticity of the PS.

Taking profit of the ability of the PS variance to quantify PS variations, this variable was used to measure the externally-induced PS shifts of the output optical signal for FRM temperatures ranging from 30°C to 65°C. The results obtained are shown in Fig. 6. In that figure, the PS variance is normalized with respect to that corresponding to a FRM temperature of 30°C. From the figure, it can be observed that, when the EDF was perturbed, the PS variance increased with FRM temperature. Thus, the PS variance at 65°C was 2.4 times bigger than the PS variance at 30 °C. This means that the birefringence effects on the PS of the output optical signal were bigger with increasing FRM temperatures because there was an increment of the rotation angle maladjustment.

4. Conclusion

In this paper the temperature dependence of FRMs and its influence on the behavior of the polarization in a R-EDFA is theoretically predicted and experimentally demonstrated. The effectiveness of the FRM gets worse with increasing temperature. As a consequence the PS shifts increase with FRM temperature when a linear birefringence is induced in the EDF. Thus, these measurements demonstrate that the FRM doesn't completely suppress the influence of external perturbations on the PS of the output optical signal. Therefore, for a stable operation of the R-EDFA polarization a temperature control at the FRM is required.

Acknowledgments

This work has been co-supported by the Spanish CICYT TIC'2001-0877-C02-01 and TEC'2004-05936-C02 projects.